Scaling Laws in PZT Thin Films Grown on Si(001) and Nb-Doped $SrTiO_3$(001) Substrates

J.-G. Ramírez, A. Cortes, W. Lopera, M. E. Gómez, and P. Prieto
Thin Film Group, Universidad del Valle A.A.25360, Cali, Colombia

Received on 8 December, 2005

A dynamic scaling and kinetic roughening study was done on digitized atomic force microscope (AFM) images of $Pb(Zr_{0.52}, Ti_{0.48})O_3$ (PZT) thin films. The films were grown on Si(001) and $Nb-SrTiO_3(001)$ (STNO) substrates via rf-sputtering technique at high oxygen pressures at substrate temperatures of 600 ^oC by varying the deposition time and keeping other growth parameters fixed. By using a specific self-designed algorithm, we can extract from digitized 512-pixel resolution AFM-images, quantitative values of roughness parameters, i.e., interface width ($\sigma(\ell)$), lateral correlation length ($\xi_{||}$) and, roughness exponent (α). Herein, we report on the sputter-time deposition dependence of the parameters describing roughness for both kinds of substrates. We report α-values for different time depositions (between 15 and 60 minutes) close to 0.55 for Si substrates and 0.63 for $Nb-SrTiO_3$ substrates, indicating that the surface becomes more correlated in STNO substrates. The α-values are associated to the Lai-Das-Sarma-Villain model.

Keywords: PZT; Thin films; AFM; Scaling laws

I. INTRODUCTION

Ferroelectric thin films are today widely used in many fields, such as nonvolatile memories, thermal or ultrasonic image sensors, and surface acoustic wave filters, since they have better distinct electric properties than those of bulk materials. Many methods, such as pulsed-laser ablation (PLD), rf-sputtering, chemical vapor deposition (CVD), metal organic decomposition (MOD), sol-gel process, and multiple electrophoretic deposition are used in the preparation of ferroelectric thin films. However, rf-sputtering has gathered considerable interest given the high quality of thin films and their relative low surface roughness. Solid films grown far from equilibrium conditions (rf-sputtering-like) are consistently predicted to have self-affine surfaces [1], and cannot be described by any equilibrium growth models. In 1985, Family and Vicsek introduced the notion of dynamic scaling to incorporate both temporal and spatial scaling behaviors [2].

$Pb(Zr_{0.52}, Ti_{0.48})O_3$(PZT) is one most promising materials for ferroelectric memory applications and has excellent ferroelectric properties with wide operating temperature range. Previous work on PZT thin films has focused on processing methods and the resulting crystallographic, electric and dielectric properties. Relatively little attention has been paid to the morphological studies in PZT thin films and less in the fractal surface analysis [3].

Surface and interface roughness are important in determining the properties and technological applicability of many systems [4]. Rough surfaces develop as a consequence of competition among different effects, such as surface tension, surface diffusion, thermal fluctuations, lattice effects, applied forces, and so on. Thus, in equilibrium, a particular surface can be rough under certain conditions and macroscopic "flat" under others. These two regimes are usually separated by a roughening transition [4,5].

Since the development of the atomic force microscope (AFM), this nondestructive technique has been used to obtain (2D,3D) images that can be characterized by a fractal approach, such as scaling laws [4,6]. In recent years, surfaces were extensively studied using scaling concepts. Statistical analysis of digitized AFM images allows for directly probing roughness, $\sigma(\ell)$, and its characteristic length scale, $\xi_{||}$.

The paper is organized as follows: We present the PZT sample preparation on Si and $Nb-SrTiO_3$ substrates followed by ex-situ AFM measurements and statistical analyses carried out upon AFM images. From statistical analyses, roughness parameters were obtained on both substrates and compared to each other.

II. EXPERIMENTAL DETAILS

A. Growth of PZT thin films and AFM analysis

PZT thin films were grown on 0.1% Nb-doped $SrTiO_3$(001) and Si(001) substrates via rf-sputtering at high oxygen pressures. A PZT target with a lead oxide (PbO) excess of 10% was necessary to compensate for the loss of this volatile component and it was used to grow stoichiometric thin films. We systematically varied deposition times (15, 30, 45, 60 minutes) and held the other deposition parameters constant. Growth temperature was at 600 ^oC, oxygen pressures was 1.1×10^{-1} mbar, and 50 watts of power in the rf-system. Each thin film was extracted for immediate *ex-situ* AFM measurements after growth. AFM images were obtained in contact mode (set point forces 1-10 nN) by using a Park Scientific Instrument AFM Microscope at room temperature and atmospheric pressure. From AFM images we extracted the value of intensity profiles ($h(\mathbf{x}, t_d)$) in a 512×512 data matrix i.e., we have information of the heights of the surface point to point in pixels for each deposition time, t_d. We developed an algorithm to calculate the corresponding local roughness from the data matrix, $\sigma_L(\ell, t_d)$, Eq.1. From these curves in log-log plot we can obtain the roughness exponent, α, correlation length, $\xi_{||}$, and the roughness saturation value, σ_{sat}.

B. Statistical treatment of images and scaling laws

In the last decade, many studies have witnessed the development of an array of theoretical tools and techniques intended to describe and characterize the roughening of non-equilibrium surfaces and interfaces. [4,7-11]. Initiated by advances in the statistical mechanics of various non-equilibrium systems, it has been observed that the roughness of many natural surfaces follows rather simple scaling laws, which can be quantified using scaling exponents. Since kinetic roughening is a common feature of sputter surfaces, before we discuss the experimental results on sputtering, we need to introduce the main quantities characterizing the surface morphology.

In thin film growth, it is not easy to have information about growth dynamics. We only have information about the final stage of the process. This information can be obtained from AFM images and they allow us to know the height function defined as $h(\mathbf{x},t_d)$; where t_d is the deposition time and $\mathbf{x}$ is any vector on the substrate. The surface is studied by using the scaling of the local roughness (local width) defined by [4,11]

$$\sigma_L^2(\ell,t_d) \equiv \left\langle [h(\mathbf{x},t_d) - h_\ell(\mathbf{x},t_d)]^2 \right\rangle_{\mathbf{x}}, \qquad (1)$$

we selected a "window" of length ℓ on the AFM image and averaged the height in this window. L is the size of the AFM image (4μm in this case). The brackets $\langle\cdots\rangle_{\mathbf{x}}$ denote spatial average over $\mathbf{x}$ direction. As ℓ increases, the local roughness, $\sigma_L(\ell,t_d)$ increases as well, and the dependence follows a power law $\sigma_L(\ell,t_d) \sim \ell^{\alpha}$ for $\ell \ll \xi_{||}(t_d)$. α is called *roughness exponent* and is a critical exponent that characterizes surface roughness. $\xi_{||}(t_d)$ defines a crossover length, sometimes called *correlation length* because it defines the limit in which the heights on surface remain correlated. For $\ell \gg \xi_{||}(t_d)$ a *saturation value*, $\sigma_{\rm sat}$, is reached [2] and becomes ℓ-independent.

Correlations can appear on surfaces due to the finite size of the substrate, and we need to quantify the length of the correlation. For $t_d \gg t_\times$ the saturation value $\xi_{||}(t_d) \sim D$, is reached, where $t_\times$ is the time to saturation and D is the substrate size.

The local roughness scales with time as $\sigma_L(\ell,t) \sim t^{\beta}$, where β is the *growth exponent*. The correlation length scales with time as $\xi_{||} \sim t^{1/Z}$, where Z is the *dynamic exponent* ($Z = \alpha/\beta$) [12].

To characterize the scaling behavior of surfaces using AFM, it is necessary to have an image set with image sizes varying a few orders of magnitude given the scale dependence of roughness. The relationship between the heights in AFM images is only given by a self-affine surface ($h(\mathbf{x},t) \sim b^{-\alpha} h(b\mathbf{x},t)$), see, for example, reference [9]. To increase critical exponent evaluation accuracy, we acquired several images for each region in the film surface and averaged all parameters. We applied the Flatter process making $\langle h(\mathbf{x},t_d)\rangle_L = 0$ before any statistical analysis of the digitized images to be sure to take into account only the fluctuations of the heights intrinsic to the surface.

Finally, the *scaling exponents* allow us to define a *universality class*, i.e. the critical exponent characterizes the $h(\mathbf{x},t)$ surface completely. These exponents are independent of system details in contrast with $\sigma_{\rm sat}$, $\xi_{||}$.

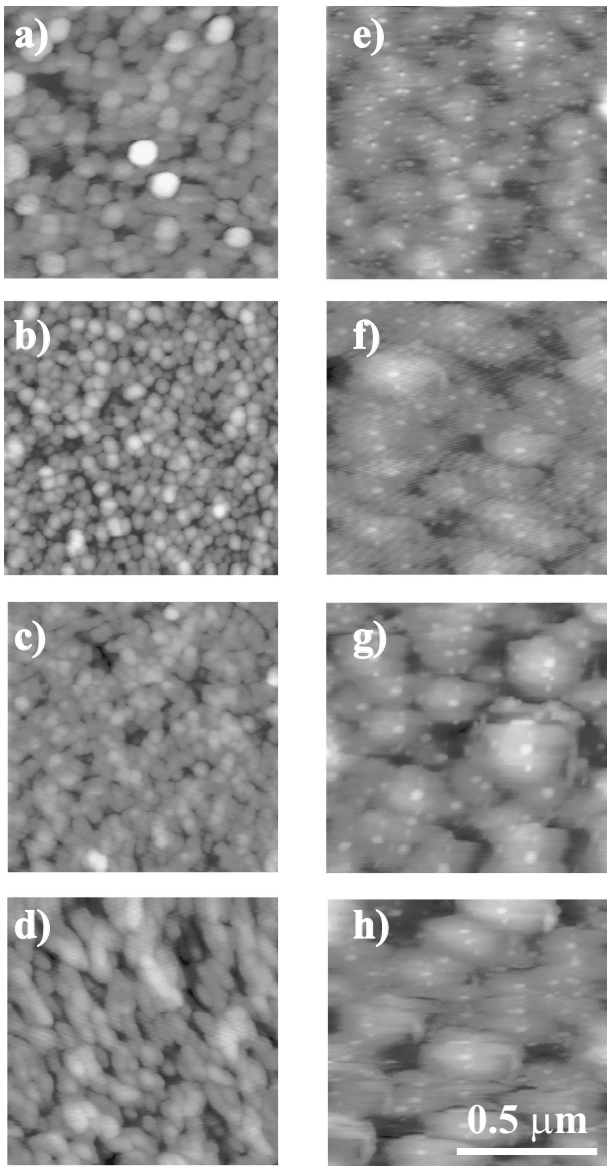

FIG. 1: AFM images of PZT on Si(001) (left column a, b, c and d) and STNO (rigt column e, f, g and h) substrates with t_d between 15 and 60 minutes (top to bottom). AFM image size is 1 μm^2.

III. RESULTS

Figure 1 shows AFM images of PZT thin films on Si (left column) and STNO (right column) substrates for each deposition time, t_d. AFM images reveal a rough microstructure formed by grains of various sizes, corresponding to column tops separated by curved (bright) regions. It is clear that grain size is homogeneous for each of the images, but for long deposition times on STNO substrates the grains become bigger. The roughness parameters were calculated using 16 μm^2 AFM images to get information on larger surface.

In Fig. 2 we show several profiles extracted from the AFM image for PZT films on STNO substrates. The dependence of the average heights to deposition times shows typical evolu-

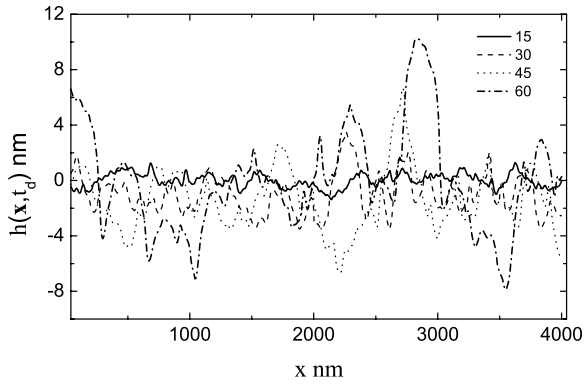

FIG. 2: Height profiles of a PZT film grown on a STNO substrate extracted from digitized AFM images for different deposition times.

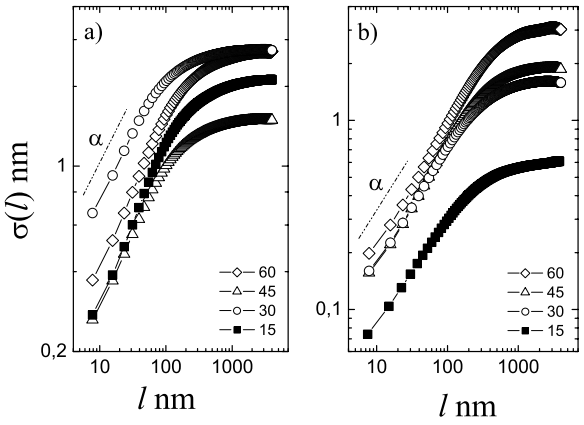

FIG. 3: Log-Log plots of *local roughness* (local width) vs local windows for PZT layers on a) Si and b) STNO substrates for 15 (■), 30 (○), 45 (△) and 60 (◊) minutes.

tion known in thin film growth. The plot shows the increase of the average heights with the increase of the deposition time.

Figure 3 shows window width ℓ dependence of the local roughness, $\sigma_L(\ell,t_d)$ in log-log plot for PZT films. Fig.3a displays the size dependent local roughness for films grown on Si substrates, and Fig.3b for those grown on STNO substrates. Each curve corresponds to different deposition times: (■) 15 min; (○) 30 min; (△) 45 min; (◊) 60 min. We just show one curve for each t_d, given that they present similar scaling behaviors. These curves exhibit self-affine typical behavior characteristic of surfaces grown in non-equilibrium processes [4]. From these curves, we obtain the *roughness exponent*, α, correlation length, $\xi_{||}$ and the saturation roughness, $\sigma_{\rm sat}$ by fitting the data to the expression $\sigma(\ell) = \sigma_{\rm sat}(1-\exp(-(\ell/\xi_{||}))^{\alpha})$ [13,14]. The quantitative values of these parameters are summarized in Table I. Interestingly enough, for the samples grown on Si substrates, the roughness exponent revealed a value of $\alpha = 0,56 \pm 0,02$; whereas, for samples grown on STNO substrates it took the value $\alpha = 0,60 \pm 0,02$. These α-values can be addressed to the Lai-Das-Sarma-Villain (LDV) model [15]:

$$\frac{\partial h}{\partial t} = R_D - \nu\nabla^4 h + \lambda\nabla^2 (\nabla h)^2 + \eta, \qquad (2)$$

where R_D is the deposition rate; the $\nu\nabla^4 h$ term accounts for smoothening by surface diffusion and is weighed by the ν parameter; the nonlinear term, $\lambda\nabla^2 (\nabla h)^2$, models the fact that steps can act as a source or sink of atoms on a growing surface and η is a stochastic roughening term. This model has scaling exponents of $\alpha \cong 2/3$, $\beta \cong 1/5$, and $Z \cong 10/3$. We could not obtain the β-exponent due to the fact that we don't not have enough points in ($\sigma_{\rm sat}$vs.t_d)-plot smaller than $t_\times$ value.

The correlation length values extracted from Fig.3 increase globally with the deposition times, indicating these heights become more correlated, i.e. although the growth process is local, information on the height of each of the neighbors spreads globally, see Table I. However, deposition time dependence of the $\sigma_{\rm sat}$ is not evident.

Figure 4a, in log-log plot, shows the saturation roughness, $\sigma_{\rm sat}$, as a function of deposition times for both series of samples: grown on t_d on STNO (○ symbols) and on Si substrates (□ symbols). For the series grown on Si substrates, we observe an anomalous behavior of the $\sigma_{\rm sat}$ with deposition times. Saturation roughness does not increase monotocally with deposition times, but decreases at characteristic time deposition and then continues increasing again. Grain size dependence of deposition time for the two series of samples is shown in Fig.4b. We observed that for the series of samples grown on STNO substrates, grain size increases with increasing deposition times, showing similar anomalous behavior for samples grown on Si substrates. This behavior may be due, probably, to mismatch between the PZT film and Si cells. The film initially grows under a given stress and for a characteristic thickness (deposition time), the stress relaxes and grain size and saturation roughness decrease. If the deposition continues, the film average roughness and grain size increase again. The roughening mechanisms of PZT thin films grown by rf-sputtering has been preliminarily studied, and our results revealed that more than one roughening mechanism is present in the growth process in addition to the stochastic and diffusion effect. From these curves β-exponent could not be obtained either.

IV. CONCLUSIONS

Self-affine scaling of PZT thin films was observed by statistical analysis of digitized AFM images. The roughness exponent was obtained for PZT films grown on Si and STNO substrates for different deposition times. The film surface becomes more correlated for PZT films grown on STNO substrates, ($\alpha \sim 0.63$), than for those grown on Si substrates, ($\alpha \sim 0.55$). The samples grown on STNO substrates showed a more homogeneous surface and lower grain size than those grown on Si substrates, for $t_d < 30$ minutes. Deposition time dependence of the saturation roughness and grain size for samples grown on Si substrates show anomalous behavior. It seems that for PZT films grown on Si substrates the stress

TABLE I: PZT Roughness parameters for Si and STNO substrates obtained from AFM images with 4μm of lateral size.

Substrate	t_d [min]	α	$\xi_{\|\|}$ [nm]	σ_{sat} [nm]	Grain size [nm]
Si	15	0,61±0,02	243±10	2,12±0,01	33
	30	0,50±0,04	135±23	2,74±0,01	37
	45	0,55±0,04	173±15	1,49±0,01	33
	60	0,58±0,03	262±11	2,70±0,01	40
$Nb-SrTiO_3$	15	0,54±0,04	303±12	0,60±0,01	20
	30	0,60±0,02	396±10	1,58±0,01	33
	45	0,65±0,02	427±10	1,94±0,01	48
	60	0,64±0,02	621±10	3,13±0,01	67

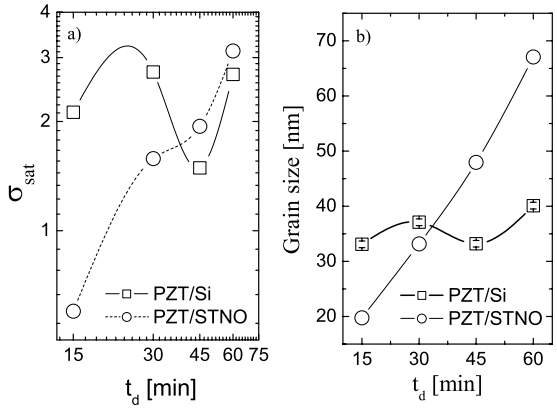

FIG. 4: Plot of grain size for PZT thin films on Si (○) and STNO substrates (□) calculated from AFM images of lateral size 1μm. The error bar of the fitted parameters has the size of the symbols. Lines are visual guides.

relaxes at deposition times ($15 < t_d < 45$). The α-values obtained were associated to LDV model.

Acknowledgments

This work has been supported by COLCIENCIAS, Colombia through the Research projects No. 1106-05-12408, 7681-05 and the Excellent Center for Novel Materials, CENM contract No 043-2005.

[1] M. G. Lagally, ed., *Fractal Growth Phenomena* (World Scientific, Singapore, 1989).
[2] F. Family and T. Vicsek, J. Phys. A **18**, L75 (1985).
[3] V. Y. Shur and et.al., Physics of the Solid State **41**, 272 (1999).
[4] A. L. Barabási and H. E. Stanley, *Fractal Concepts in Surface Growth* (Cambridge - University Press, Cambridge, 1995).
[5] S. A. Safran, *Statistical Thermodynamics of Surfaces, Interfaces, and Membranes* (Addison Wesley, Reading, MA, 1994).
[6] P. Klapeteck and I. Ohldal, Ultramicroscopy **94** (2003).
[7] M. A. Makeev, Nuc. Inst. Meth. Phys. Res. B **197**, 185 (2002).
[8] P. Meakin, Phys. Rep. **235**, 189 (1990).
[9] M. E. R. Dotto and M. U. Kleinke, Phys. Rev. B **65**, 245323 (2002).
[10] D. Lu and et. al., Phys. Lett. A **78**, 82 (2004).
[11] J. G. Ramírez and et.al., Physica Status Solidi (c) **1**, S13 (2004).
[12] F. Family, Physica A **168**, 561 (1990).
[13] J. Santamaria, M. E. Gomez, J. L. Vicent, K. M. Krishnan, and I. K. Schuller, Phys. Rev. Lett. **89**, 1 (2002).
[14] S. K. Sinha, E. B. S. S. Garoff, and H. B. Stanley, Phys. Rev. B **38**, 2297 (1988).
[15] Z. W. Lai and S. D. Sarma, Phys. Rev. Lett. **66**, 2348 (1991).